ACS APPLIED MATERIALS & INTERFACES

www.acsami.org

Research Article

Ultrasensitive Poly(boric acid) Hydrogel-Coated Quartz Crystal Microbalance Sensor by Using UV Pressing-Assisted Polymerization for Saliva Glucose Monitoring

Qian Dou, Zifeng Zhang, Yanxiang Wang, Shiwen Wang, Debo Hu, Zhipeng Zhao, Hongliang Liu,* and Qing Dai*

Cite This: *ACS Appl. Mater. Interfaces* 2020, 12, 34190−34197

Read Online

ACCESS | Metrics & More | Article Recommendations | Supporting Information

ABSTRACT: Quartz crystal microbalance (QCM) has attracted extensive attention in the field of biological analysis and detection because of its high sensitivity, fast response, real-time measurement, good operability, and low-cost production. However, to detect the trace amounts of small molecules, such as low-concentration saliva glucose under physiological conditions, is still a major challenge. Herein, the surface of a QCM chip was coated with a poly(boric acid)-based hydrogel using UV pressing-assisted polymerization to obtain a simple device for glucose detection. The designed QCM sensor shows a record-low detection limit of glucose (3 mg/L at pH 7.5), which is ∼30 times lower than that of sensors fabricated by conventional surface initiation−spin coating. The outperformance of the poly(boric acid) hydrogel-coated QCM sensor is probably due to the uniform and compact microstructure, as well as the presence of sufficient glucose-binding sites resulting from the hydrogel coating generated by UV pressing-assisted polymerization. This method provides an important solution to detect the trace amounts of small organic molecules or ions and has the potential to push forward the practical applications of QCM sensors.

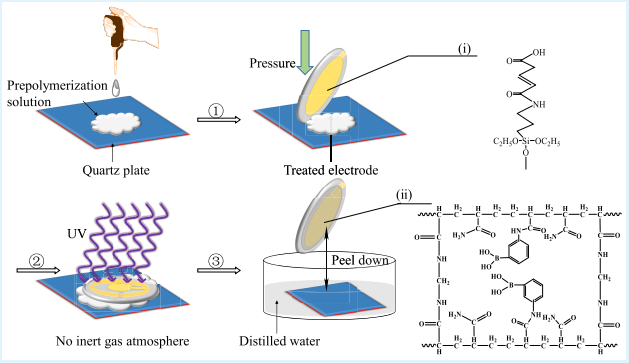

KEYWORDS: *glucose, QCM, UV pressing, hydrogel, adsorption*

1. INTRODUCTION

Quartz crystal microbalance (QCM) is a very sensitive detector that can detect subnano mass changes.[1−3] Owing to its high sensitivity, fast response, low-cost production, ability of real-time measurement, and simple integration compared with other electronic components, QCM is considered as an important microbiosensor in the field of biological analysis and detection.[4−9] Current research on QCM focuses on the exploration of mechanism and kinetics of binding processes of large biomolecules,[10,11] as well as the detection of DNA,[12,13] proteins,[14,15] bacteria,[16] etc. In addition, recent reports have examined the application of QCMs in reproductive medicine, e.g., the in situ assessment of the postejaculatory dynamics of human seminal fluids (viscosity, volume, and sperm concentration).[17,18] Furthermore, only a few of reports focus on the detection of organic molecules and ions with QCM in liquids.[19]

In 2019, ∼463 million people diagnosed with diabetes worldwide (aged 20−79), and the number of diabetics will reach 578.4 million by 2030. Diabetes and its complications impose significant economic consequences for individuals, families, health systems, and countries. The American Diabetes Association (ADA) has conclusively shown that self-monitoring of blood glucose (SMBG) is an important part of diabetes management and individualized treatment. SMBG results are helpful to evaluate the degree of glucose metabolism disorder in patients with diabetes, develop a reasonable hypoglycemic program, and reflect the effect of hypoglycemic treatment, which allows appropriate adjustment of the hypoglycemic program.[20,21] However, the inconvenience, expense, pain, and complexity involved in SMBG lead to its underutilization.[22,23] Therefore, an accurate, painless, and easy-to-use device is urgently needed to achieve glucose monitoring. Reports have shown that glucose concentration in saliva is highly correlated with blood sugar levels.[24−26] Therefore, saliva has become an ideal marker for noninvasive blood glucose monitoring because of its safety, noninvasiveness, convenience, and real-time monitoring.[27,28] However, the concentration of glucose in saliva is extremely low, accounting for ∼1/100−1/50 of the

Received: May 5, 2020
Accepted: June 23, 2020
Published: June 23, 2020

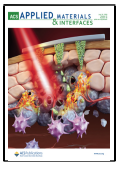

https://dx.doi.org/10.1021/acsami.0c08229
ACS Appl. Mater. Interfaces 2020, 12, 34190−34197

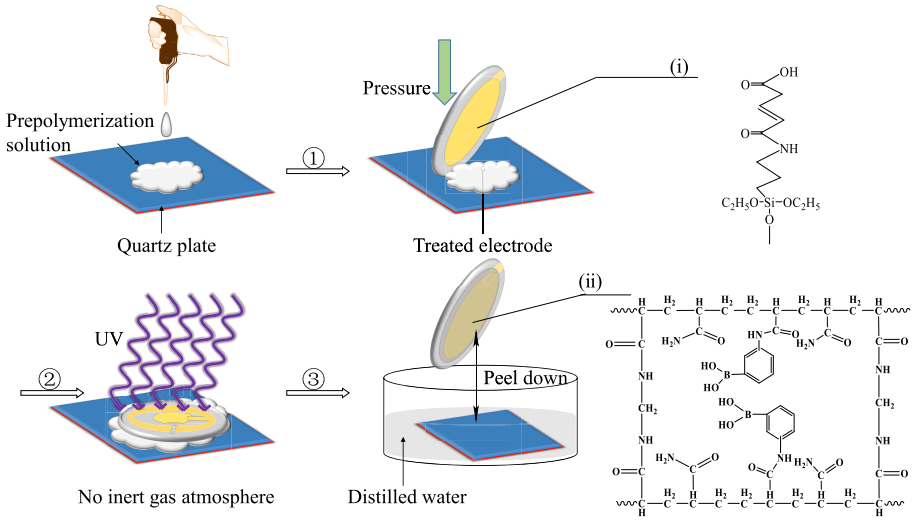

Figure 1. Synthesis of hydrogel-coated QCM electrode by UV pressing. ① Dropping of the prepolymerized solution onto the electrode surface and application of external pressure. ② UV polymerization. ③ Peeling off of the hydrogel-coated QCM sensor from the working solid substrate-crystal plate.

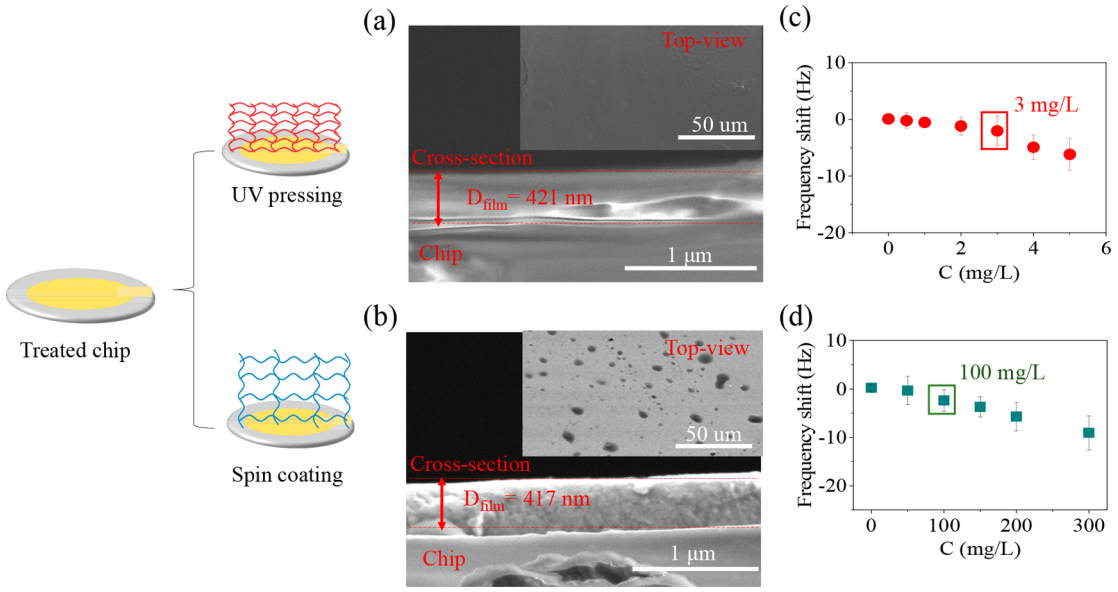

Figure 2. Comparison of hydrogel-coated QCM electrodes prepared by different methods. (a) Hydrogel coating fabricated by UV pressing exhibited a uniform and dense structure. (b) Hydrogel coating generated by spin-coating showed a heterogeneous structure with obvious spots. The hydrogel-coated QCM sensors synthesized by UV pressing and spin-coating can achieve the detection limit of 3 mg/L (c) and 100 mg/L (d), separately.

blood glucose concentration. In addition, glucose is a small-molecule monosaccharide (MW = 180.16 g/mol). Therefore, changes of the glucose concentration in saliva cause only a small signal, which is difficult to be detected by QCM. This presents a critical factor that limits applications of glucose-QCM sensors.[29,30]

To achieve low-concentration saliva glucose detection under physiological conditions, a glucose-sensitive, film-coated QCM electrode with high specific adsorption is desirable. Compared with conventional glucose-responsive materials, such as enzymes and lectins, boric acid polymers benefit from their stability, durability, low cost, and high glucose sensitivity and are widely used in glucose-identification materials.[31−33] QCM electrodes are coated with polymers via chemical methods, where the initiator is fixed on the surface of the QCM electrode, and the polymer is subsequently grown in situ on its surface via free radical polymerization.[34,35] However, the number of sensors based on QCM are sensitive enough to steadily detect low-concentration glucose in saliva (20−200 μmol/L; after conversion, 3.6−36 mg/L)[36] under physiological conditions is quite limited (Table S2 in the Supporting Information).

Herein, a new method of coating poly(boric acid) hydrogel onto the surface of a QCM electrode by UV pressing-assisted polymerization was demonstrated (denoted as UV pressing). The functional poly(boric acid) hydrogel coating obtained by this method has many merits, such as a dense structure, sufficient glucose-binding sites, excellent stability, good uniformity and easy to operate. Inert gas atmosphere is not required during the UV-induced reaction, which simplifies the

https://dx.doi.org/10.1021/acsami.0c08229
ACS Appl. Mater. Interfaces 2020, 12, 34190−34197

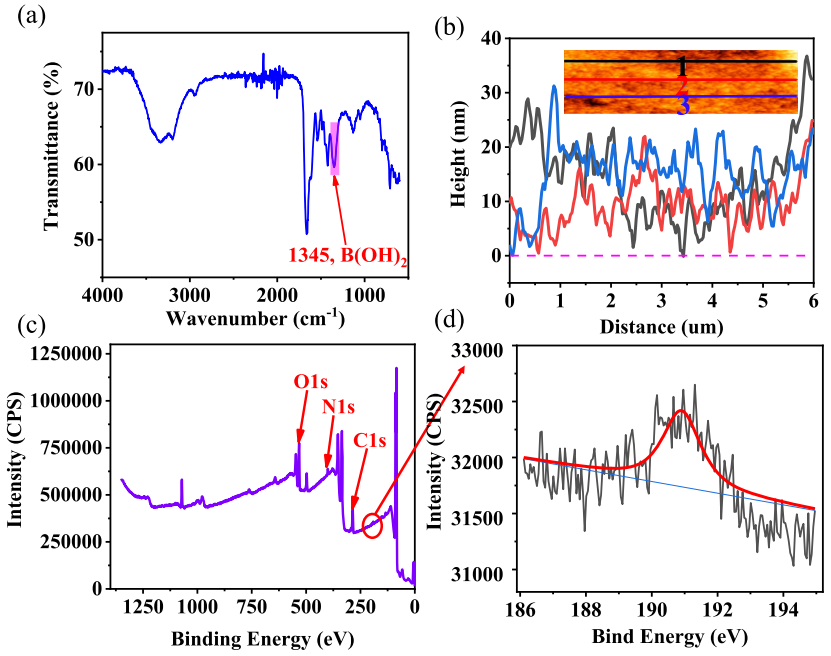

Figure 3. (a) FTIR spectrum of hydrogel-coated electrode. (b) Homogenous hydrogel surface (peak−valley roughness ∼35 nm). (c) XPS survey scan of hydrogel-coated chip. (d) B 1s signal at 191 eV is attributed to the boric acid groups (black line, actual measurement; red line, Gaussian fit through the XPS data; blue line, software-generated baseline of Gaussian fit).

experimental process and saves resources. In combination with our lab-built QCM platform, glucose can be successfully detected in phosphate-buffered saline (PBS) and artificial saliva under physiological conditions, and a glucose detection limit of 3 mg/L was obtained at pH 7.5. This work provides a new method for detecting low concentrations of small molecules based on QCM.

2. RESULTS AND DISCUSSION

2.1. Synthesis of the Hydrogel. A polymerizable double bond was grafted onto the upper side of the QCM electrode (Figure 1(i) and Figure S1). The synthesis of the surface-grafted hydrogel on the electrode can be roughly divided into three steps (Figure 1). First, a clean quartz plate was prepared, and a small amount of prepolymerization solution was dropped onto the quartz plate. Then, the treated QCM electrode was placed face down on the prepolymerization solution, and the bottom side was pressed with uniform force. After exposure to ultraviolet light for a short time, the hydrogel formed on the electrode surface. Finally, the hydrogel-coated QCM (Figure 1(ii)) was separated from the working solid substrate-crystal plate by immersion in distilled water.

Films synthesized by two different methods (UV pressing and surface initiation−spin coating) were analyzed by scanning electron microscopy (SEM), as presented in Figure 2. Figure 2a (top view) shows that the surface of the hydrogel synthesized by UV pressing was complete and relatively flat. In contrast, Figure 2b (top view) reveals that the film synthesized by spin-coating is not complete and exhibits many spots (SEM image of the double-bonded QCM chip is shown in Figure S3). Parts a and b of Figure 2 (cross section) show that the hydrogel synthesized by UV pressing is more compact, which will increase the amount of boric acid groups in the hydrogel. The thickness of the prepared films by either method is ∼420 nm.

To prove the superiority of UV pressing, the detection limits of hydrogel-coated QCM sensors prepared by both methods were studied by a lab-built QCM platform (Figure S10). In this work, the detection limit refers to the minimum glucose concentration that can be detected by a boric acid hydrogel-coated QCM sensor (Figure S6). As described earlier, parts c and d of Figure 2 show that the detection limit of the hydrogel-coated QCM sensor prepared by UV pressing is 3 mg/L, which is significantly lower than the detection limit of 100 mg/L determined for the sensor prepared by spin-coating. This indicates that the film prepared by UV pressing has a better glucose response.

The main reason for the excellent glucose-binding performance of the hydrogel prepared by UV pressing is the external pressure applied during the fabrication process. Because the prepolymerized solution is confined between the electrode and the quartz plate, the hydrogel formed by polymerization possesses uniformity and compact microstructures. In addition, the polymerization does not require inert gas protection, as the air in the prepolymerization liquid is eliminated by the applied pressure. Other advantages include the facile synthesis process and the possibility to control the thickness of the hydrogel by tuning the applied pressure (see Figure S9).

2.2. Characterization. The hydrogel-coated electrode was characterized by fourier transform infrared (FTIR). As shown in Figure 3a, the peak at ∼3195 cm^{-1} is attributed to the N−H stretching vibration of the NH_2 group, and the peak at ∼1658 cm^{-1} is attributed to the C═O stretching vibration.[37] Characteristic absorption peak of C_6H_6 appears at ∼1423 cm^{-1},[38] and the absorption peak at ∼1345 cm^{-1} is assigned to B−O.[39] These results confirm the formation of the boric acid hydrogel.

The surface roughness of the hydrogel-coated electrode was analyzed by atomic force microscopy (AFM). The results show that the surface of the hydrogel is homogeneous (peak−valley roughness ∼35 nm, Figure 3b). SEM and AFM analyses of

https://dx.doi.org/10.1021/acsami.0c08229
ACS Appl. Mater. Interfaces 2020, 12, 34190−34197

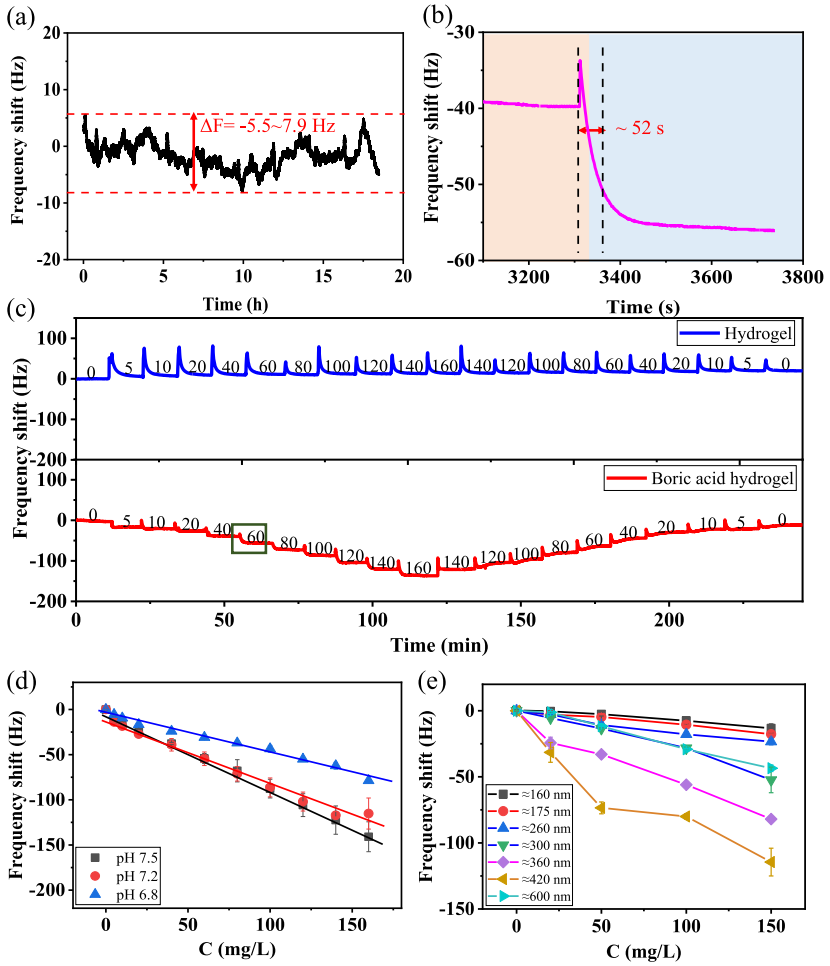

Figure 4. (a) Hydrogel-coated QCM sensor shows a tiny fluctuation of ∼13 Hz in PBS (pH 7.5) for at least 20 h. (b) Response time of the sensor in the detection of glucose of 52 s in PBS at pH 7.5. (c) Control hydrogel (in the absence of 3-APB) showing no frequency change, and hydrogel prepared with 3-APB showing a good response to different concentrations of glucose in PBS at pH 7.5 (glucose concentration increasing from 0 to 160 mg/L and then decreasing from 160 to 0 mg/L). (d) Favorable linear relationship between frequency shifts and different glucose concentrations (from 0 to 160 mg/L) in PBS from pH 6.8 to pH 7.5. (e) Impact of hydrogel thickness on glucose detection, revealing an optimal hydrogel thickness of ∼260 nm without considering the effect of film swelling.

hydrogel-coated chip in dry state and glucose solution are shown in Figure S4a−d.

Figure 3c shows an X-ray photoelectron spectroscopy (XPS) survey scan of the hydrogel-coated electrode, where the peaks of C 1s, O 1s, and N 1s are attributed to various reactants (3-acrylamidophenylboronic acid, acrylamide, and *N*,*N*′-methylenebis(acrylamide)). The B 1s signal at 191 eV indicates the presence of boric acid groups (Figure 3d).[40,41] The element distributions of B 1s, C 1s, and O 1s are 6.6 ± 1.7%, 43.5 ± 2.0%, and 24.8 ± 1.4%, respectively.

2.3. Hydrogel Properties. The performance of the hydrogel was studied in PBS, and the resonant frequency shift ($\triangle F$ = F(glucose sample) − F(blank sample)) was measured to evaluate the glucose sensor performance. First, the stability of the sensor, which presents a very important aspect of the performance, was tested. The hydrogel-coated QCM electrode was placed in a flow cell, and PBS was injected by a peristaltic pump at room temperature. The hydrogel-coated QCM sensor showed a tiny fluctuation of ∼13 Hz in PBS for ∼20 h (Figure 4a).

Boric acids can covalently bind to glucose and reversibly form a boric acid diester (Figure S2a).[42,43] A hydrogel-coated QCM sensor can recognize glucose molecules (Figure S2b). For a control experiment, the hydrogel was synthesized under the same conditions as the boric acid hydrogel without 3-(acrylamido) phenylboronic acid (3-APB) in the prepolymer solution. As shown in Figure 4c, as the glucose concentration changed, the $\triangle F$ of the control hydrogel did not show any obvious changes. In contrast, the boric acid hydrogel showed $\triangle F$ response to glucose in the concentration range of 0−160 mg/L, which encompasses the concentration range of glucose in saliva of both healthy people and diabetics.[44] When the glucose concentration gradually increased from 0 to 160 mg/L, the absolute value of $\triangle F$ increased rapidly, suggesting rapid binding between boric acid groups of the hydrogel and glucose molecules. With increasing reaction time, $\triangle F$ gradually stabilized. As the glucose concentration gradually decreased from 160 to 0 mg/L, the absolute value of $\triangle F$ gradually decreased, indicating that glucose molecules were released from the hydrogel (detection under different pH values is shown in Figure S8). These results indicate that 3-APB in the hydrogel is the active molecule that binds glucose in solution. The response time is defined as the time when 90% of the total frequency shift is achieved.[45,46] Magnification of the data (Figure 4c, green box) shows a fast response of the hydrogel to glucose of ∼52 s (Figure 4b).

https://dx.doi.org/10.1021/acsami.0c08229
ACS Appl. Mater. Interfaces 2020, 12, 34190−34197

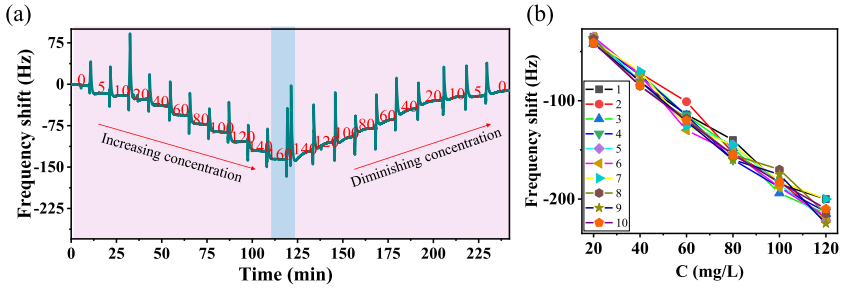

Figure 5. (a) Sensor showing a good response to different concentrations of glucose in artificial saliva at pH 7.5 (glucose concentration increasing from 0 to 160 mg/L and then decreasing from 160 to 0 mg/L). (b) Frequency shifts that remained largely stable during repeated testing (10 measurements) of artificial saliva containing different glucose concentrations with the hydrogel-coated sensor at pH 7.9.

In addition, the pH value of the detection medium plays an important role for the binding ability of the hydrogel. Figure 4d shows the sensor response to glucose in the concentration range of 0−160 mg/L at different pH values, revealing a favorable linear relationship between glucose concentration and $\triangle F$ at pH values of 6.8−7.5 (physiological pH range of human saliva). With increasing pH, the absolute value of $\triangle F$ increased due to the higher pH promoting ionization of boric acid and increasing the number of glucose molecules that bind to boric acids. Glucose concentration and $\triangle F$ are linearly correlated with linear correlation coefficients of 0.9532, 0.9393, and 0.9858 at pH 6.8, 7.2, and 7.5, respectively.

Furthermore, the influence of the hydrogel thickness on $\triangle F$ was studied. Upon increasing the film thickness from 160 to 420 nm at a constant glucose concentration, the absolute value of $\triangle F$ increased (Figure 4e). In contrast, when the film thickness increased to 600 nm, the absolute value of $\triangle F$ decreased ($\triangle F$, $\triangle R$, and $\triangle M$ data are shown in Figure S7a−c).

2.4. Artificial Saliva Test. The prepared glucose sensor was then used to detect glucose in artificial saliva to further evaluate the performance of the hydrogel. As shown in Figure 5a, the absolute value of $\triangle F$ increased with increasing glucose concentration. Conversely, the absolute value of $\triangle F$ gradually decreased with decreasing glucose concentration. Furthermore, the hydrogel recovered well, which is comparable to the results obtained in PBS buffer solution.

As presented in Figure 5a, the absolute value of $\triangle F$ was relatively small between pH 6.8 and 7.5. As the pH value increased, the absolute value of $\triangle F$ gradually became larger (Figure 4d). Therefore, the pH was adjusted to 7.9 to increase the signal value. (At pH ≥ 8.0, the baseline fluctuation of the sensor was unstable. Fluctuations of $\triangle F$ were almost twice as high as that at pH 7.5 (Figure S5)). No significant changes were observed when each glucose sample was tested 10 times, as shown in Figure 5b (R^2 = 0.9979). The RSD (relative standard deviation) of each glucose concentration was <10% (Table S1). This experiment proved the high stability and accuracy of the hydrogel.

3. CONCLUSIONS

The fabrication of an ultrasensitive poly(boric acid) hydrogel-coated QCM electrode by UV pressing and its application as a sensor for the detection of glucose are reported. The hydrogel coating has many merits, like a dense structure, sufficient glucose-binding sites, excellent stability and good uniformity. These unique properties endow the QCM sensor with a record-low glucose detection limit under physiological conditions, making it suitable for saliva glucose monitoring. QCM measurements revealed that the glucose detection limit is as low as 3 mg/L, and the detection range of glucose is 0−160 mg/L with good linearity in the range of pH 6.8−7.5. Repeated glucose tests of artificial saliva showed negligible deviations between measurements, indicating good reproducibility (RSD < 10%, n = 10, pH = 7.9). In follow-up studies, the hydrogel-coated QCM sensor will be gradually optimized for glucose detection in real saliva.

4. EXPERIMENTAL DESIGN AND PROCEDURE

4.1. Instruments and Reagents. *Instruments.* The QCM chips were purchased from the SiYi Coating Material Business Department of Danyang Development Zone. The fundamental frequency of the QCM chip is 5 MHz, and it has a gold electrode surface. Glucose tests were performed using QCM 200 (SRS) and a lab-built QCM platform. Surface morphologies and material thicknesses of the hydrogels were investigated by scanning electron microscopy (S-4800 and SU8220). The hydrogel surface morphologies in glucose solution were investigated by environmental scanning electron microscopy (HD-Q-200) and atomic force microscopy (M8-HR). The functional groups of the hydrogel were characterized by microinfrared spectrometry (SP-200i), and the transmission was measured by attenuated total reflection. The chemical composition of the hydrogel was analyzed by X-ray photoelectron spectrometry (ESCALAB250-Xi). The surface roughness of the hydrogel was analyzed by atomic force microscopy using Neaspec s-SNOM. During the preparation of the cross-linked polymer films, pressure was applied using a tailor-made pressure film machine. Ultraviolet polymerization at 365 nm was induced using a UV lamp.

Reagents. Acrylamide (AM, 98.5%) was purchased from Xilong Chemical Co., Ltd., 2,2-dimethoxy-1,2-diphenylethanone (DMPA, > 98%) was purchased from TCI Development Co., Ltd. (Shanghai), 3-aminopropyltriethoxysilane (APTES, 98%) was purchased from Alfa Aesar Chemicals Co., Ltd. (China), 3-(acrylamido)phenylboronic acid (3-APB, 98%) was purchased from Frontier Scientific, *N*,*N*′-methylenebis(acrylamide) (BIS, 98%) was purchased from Sinopharm Chemical Reagent, Ltd., and glucose (99.8%) was purchased from National Institutes for Food and Drug Control. Dimethyl sulfoxide (DMSO), glucose, sodium phosphate dibasic dodecahydrate, potassium dihydrogen phosphate, and maleic anhydride were all purchased as pure analytical reagents.

Preparation of PBS. First, 35.82 g of $Na_2HPO_4{\cdot}12H_2O$ was dissolved in 1 L of distilled water, and 7.8 g of $KH_2PO_4{\cdot}2H_2O$ was dissolved in 500 mL of distilled water. Then, 770 mL of Na_2HPO_4 solution and 230 mL of KH_2PO_4 solution were mixed to obtain the required PBS solution. The pH was adjusted using NaOH and HCl solution.

Preparation of Artificial Saliva According to ISO 10271−2011.[47] The specific composition of artificial saliva is 0.4 g/L NaCl, 0.795 g/L $CaCl_2{\cdot}H_2O$, 0.4 g/L KCl, 0.005 g/L $Na_2S{\cdot}2H_2O$, 0.78 g/L $Na_2HPO_4{\cdot}12H_2O$, 1 g/L urea, and 1 L of PBS. NaOH and HCl were added to

https://dx.doi.org/10.1021/acsami.0c08229
ACS Appl. Mater. Interfaces 2020, 12, 34190−34197

adjust the pH. The obtained artificial saliva was filtered through a poly(ether sulfone) membrane with a pore size of 0.22 μm.

4.2. Hydrogel Synthesis. *Surface Modification of QCM Electrode.* A QCM electrode was sonicated for 10 min in piranha solution (mixture of H_2SO_4 (96%, w/w) and H_2O_2 (30%, w/w) in a volume ratio of 7:3). The processed electrode was washed with redistilled water and dried with N_2 gas. Then, the electrode was immersed in a mixed solution of 3-aminopropyltriethoxysilane (100 μL) and ethanol (50 mL) at room temperature. After 12 h, the electrode was rinsed with ethanol and subsequently dried with N_2 gas. The dried electrode was immersed in a mixed solution of maleic anhydride (1 g) and *N*,*N*′-dimethylformamide (50 mL) for 12 h. Finally, the treated electrode was rinsed with ethanol and dried with N_2 gas.[48,49]

Hydrogel Film Synthesis by UV Pressing. First, 5 mol/L prepolymer solution was prepared, which consisted of 18 wt % 3-APB, 2 wt % BIS, 78 wt % AM, and 2 wt % DMPA in dimethyl sulfoxide. Second, 25 μL of prepolymerization solution was dropped onto a quartz plate (10 × 10 cm). The electrode was placed face down on the prepolymerization solution and pressed with appropriate force. The crystal plate was irradiated with a UV lamp (λ = 365 nm) for 30 min. Then, the crystal plate was placed in distilled water for ∼1 h to automatically detach the hydrogel-coated QCM sensor from the working solid substrate-crystal plate. Finally, the film-coated electrode was rinsed with redistilled water. For comparison, a control hydrogel was synthesized according to the same procedure without addition of 3-APB.

Hydrogel Synthesis by Spin-Coating. Electrode pretreatment and formulation of the prepolymerized solution were the same as described earlier for the hydrogel synthesis by UV pressing. Then, 50 μL of prepolymer solution was deposited onto the electrode and spin-coated for 1 min at 3000 rpm. The electrode coated with the prepolymer was placed in a customized glass container that was repeatedly evacuated to remove O_2. For polymerization, the electrode was irradiated with UV light (λ = 365 nm) under N_2 atmosphere for 30 min. Finally, the obtained film-coated QCM electrode was repeatedly rinsed with redistilled water.

Glucose Detection with Hydrogel-Coated QCM Sensor. A QCM chip coated with a glucose-sensitive hydrogel was dried with nitrogen and installed into the reaction cell of the QCM. PBS was pumped into the reaction cell using a peristaltic pump, and the frequency of the QCM chip was monitored in real time using the QCM data-acquisition software. After $\triangle F$ was stabilized, the glucose detection capacity of the hydrogel was evaluated. During the test, the glucose solution (2 mL) was injected with a flow of 200 μL/s. When the glucose solution was fully injected into the reaction cell, the peristaltic pump was closed. After $\triangle F$ stabilized, the next sample was injected.

■ ASSOCIATED CONTENT

Supporting Information

The Supporting Information is available free of charge at https://pubs.acs.org/doi/10.1021/acsami.0c08229.

> Synthesis of the hydrogel, glucose binding to the hydrogel, SEM of treated QCM chip, SEM and AFM of hydrogel-coated chip, fluctuation of the frequency shift at pH 8.0, detection limit, resistance and mass displacement, glucose response at different pH values, data stability, pressure membrane process, physical map of glucose sensor, and comparison with literature (PDF)

■ AUTHOR INFORMATION

Corresponding Authors

Hongliang Liu − *CAS Key Laboratory of Bio-Inspired Materials and Interfacial Science, Technical Institute of Physics and Chemistry, Chinese Academy of Sciences, Beijing 100190, P. R. China;* orcid.org/0000-0002-6781-3546; Email: liuhl@mail.ipc.ac.cn

Qing Dai − *Division of Nanophotonics, CAS Key Laboratory of Standardization and Measurement for Nanotechnology, CAS Center for Excellence in Nanoscience, National Center for Nanoscience and Technology, Beijing 100190, P. R. China; School of Materials Science and Engineering, Zhengzhou University, Zhengzhou 450001, P. R. China; Center of Materials School and Optoelectronics, University of Chinese Academy of Scienses, Beijing 100049, P. R. China;* orcid.org/0000-0002-1750-0867; Email: daiq@nanoctr.cn

Authors

Qian Dou − *Division of Nanophotonics, CAS Key Laboratory of Standardization and Measurement for Nanotechnology, CAS Center for Excellence in Nanoscience, National Center for Nanoscience and Technology, Beijing 100190, P. R. China; School of Materials Science and Engineering, Zhengzhou University, Zhengzhou 450001, P. R. China*

Zifeng Zhang − *Division of Nanophotonics, CAS Key Laboratory of Standardization and Measurement for Nanotechnology, CAS Center for Excellence in Nanoscience, National Center for Nanoscience and Technology, Beijing 100190, P. R. China; School of Materials Science and Engineering, Zhengzhou University, Zhengzhou 450001, P. R. China*

Yanxiang Wang − *Institute of Medicinal Biotechnology, Chinese Academy of Medical Sciences and Peking Union Medical College, Beijing 100050, P. R. China*

Shiwen Wang − *Division of Nanophotonics, CAS Key Laboratory of Standardization and Measurement for Nanotechnology, CAS Center for Excellence in Nanoscience, National Center for Nanoscience and Technology, Beijing 100190, P. R. China*

Debo Hu − *Division of Nanophotonics, CAS Key Laboratory of Standardization and Measurement for Nanotechnology, CAS Center for Excellence in Nanoscience, National Center for Nanoscience and Technology, Beijing 100190, P. R. China*

Zhipeng Zhao − *Division of Nanophotonics, CAS Key Laboratory of Standardization and Measurement for Nanotechnology, CAS Center for Excellence in Nanoscience, National Center for Nanoscience and Technology, Beijing 100190, P. R. China*

Complete contact information is available at: https://pubs.acs.org/10.1021/acsami.0c08229

Funding

This work was supported by the Science and Technology Service Network Project (STS Program) of the Chinese Academy of Sciences (KFJ-STS-ZDTP-063), the National Key Research and Development Program of China (2016YFA0201600), the National Natural Science Foundation of China (Grant No. 51925203), and the Ministry of Science and Technology focused on the research of "Early Identification, Early Diagnosis, and Cutting Point of Diabetes Risk Factors" (2016YFC1305700). The work was further funded by the Jiangsu Provincial Basic Public Health Service Innovation Pilot Project (WDF15-967) and the Jiangsu Medical Device Industry Technology Innovation Center Joint Fund (SYC2018004).

Notes

The authors declare no competing financial interest.

REFERENCES

(1) Furusawa, H.; Sekine, T.; Ozeki, T. Hydration and Viscoelastic Properties of High- and Low-Density Polymer Brushes Using a Quartz-Crystal Microbalance Based on Admittance Analysis (QCM-A). *Macromolecules* **2016**, *49*, 3463−3470.

(2) Zhang, Z.; Fan, J.; Yu, J. M.; Zheng, S. R.; Chen, W. J.; Li, H. G.; Wang, Z. J.; Zhang, W. G. New Poly(N,N-Dimethylaminoethyl Methacrylate)/Polyvinyl Alcohol Copolymer Coated QCM Sensor for Interaction with CWA Simulants. *ACS Appl. Mater. Interfaces* **2012**, *4*, 944−949.

(3) Chen, H. B.; Su, X. D.; Neoh, K.-G.; Choe, W.-S. QCM-D Analysis of Binding Mechanism of Phage Particles Displaying a Constrained Heptapeptide with Specific Affinity to SiO_2 and TiO_2. *Anal. Chem.* **2006**, *78*, 4872−4879.

(4) Webster, A.; Vollmer, F.; Sato, Y. Probing Biomechanical Properties with a Centrifugal Force Quartz Crystal Microbalance. *Nat. Commun.* **2014**, *5*, 5284.

(5) Benito, J.; Sorribas, S.; Lucas, I.; Coronas, J.; Gascon, I. Langmuir−Blodgett Films of the Metal−Organic Framework MIL101(Cr): Preparation, Characterization, and CO_2 Adsorption Study Using a QCM-Based Setup. *ACS Appl. Mater. Interfaces* **2016**, *8*, 16486−16492.

(6) Fukao, N.; Kyung, K.-H.; Fujimoto, K.; Shiratori, S. Automatic Spray-LBL Machine Based on in-Situ QCM Monitoring. *Macromolecules* **2011**, *44*, 2964−2969.

(7) Tsuge, Y.; Moriyama, Y.; Tokura, Y.; Shiratori, S. Silver Ion Polyelectrolyte Container as a Sensitive Quartz Crystal Microbalance Gas Detector. *Anal. Chem.* **2016**, *88*, 10744−10750.

(8) Eisele, N. B.; Andersson, F. I.; Frey, S.; Richter, R. P. Viscoelasticity of Thin Biomolecular Films: A Case Study on Nucleoporin Phenylalanine-Glycine Repeats Grafted to a Histidine-Tag Capturing QCM-D Sensor. *Biomacromolecules* **2012**, *13*, 2322−2332.

(9) Handley, J. Product Review: Quartz Crystal Microbalances. *Anal. Chem.* **2001**, *73*, 225A−229A.

(10) Cho, N.-J.; Frank, C. W.; Kasemo, B.; Höök, F. Quartz Crystal Microbalance with Dissipation Monitoring of Supported Lipid Bilayers on Various Substrates. *Nat. Protoc.* **2010**, *5*, 1096−1106.

(11) Molino, P. J.; Yue, Z. L.; Zhang, B. B.; Tibbens, A.; Liu, X.; Kapsa, R. M. I.; Higgins, M. J.; Wallace, G. G. Influence of Biodopants on PEDOT Biomaterial Polymers: Using QCM-D to Characterize Polymer Interactions with Proteins and Living Cells. *Adv. Mater. Interfaces* **2014**, *1*, 1300122.

(12) Jin, Y. L.; Xie, Y. F.; Wu, K.; Huang, Y. Y.; Wang, F. Y.; Zhao, R. Probing the Dynamic Interaction between Damaged DNA and a Cellular Responsive Protein Using a Piezoelectric Mass Biosensor. *ACS Appl. Mater. Interfaces* **2017**, *9*, 8490−8497.

(13) Rawle, R. J.; Johal, M. S.; Selassie, C. R. D. A Real-Time QCM-D Approach to Monitoring Mammalian DNA Damage Using DNA Adsorbed to a Polyelectrolyte Surface. *Biomacromolecules* **2008**, *9*, 9−12.

(14) Luan, Y. F.; Li, D.; Wei, T.; Wang, M. M.; Tang, Z. C.; Brash, J. L.; Chen, H. "Hearing Loss" in QCM Measurement of Protein Adsorption to Protein Resistant Polymer Brush Layers. *Anal. Chem.* **2017**, *89*, 4184−4191.

(15) Noi, K.; Iwata, A.; Kato, F.; Ogi, H. Ultrahigh-Frequency, Wireless MEMS QCM Biosensor for Direct, Label-Free Detection of Biomarkers in a Large Amount of Contaminants. *Anal. Chem.* **2019**, *91*, 9398−9402.

(16) Perez-Anes, A.; Szarpak-Jankowska, A.; Jary, D.; Auzély-Velty, R. β-CD-Functionalized Microdevice for Rapid Capture and Release of Bacteria. *ACS Appl. Mater. Interfaces* **2017**, *9*, 13928−13938.

(17) Esmeryan, K. D.; Ganeva, R. R.; Stamenov, G. S.; Chaushev, T. A. Superhydrophobic Soot Coated Quartz Crystal Microbalances: A Novel Platform for Human Spermatozoa Quality Assessment. *Sensors* **2019**, *19* (1), 123.

(18) Esmeryan, K. D.; Stamenov, G. S.; Chaushev, T. A. An Innovative Approach for In-Situ Detection of Postejaculatory Semen Coagulation and Liquefaction Using Superhydrophobic Soot Coated Quartz Crystal Microbalances. *Sensor Actuat A-Phys.* **2019**, *297*, 111532.

(19) Ma, W. Y.; Tang, S.; Wei, Y. H.; Xie, G. Z. Simple Biosensing Method to Detect DMMP Based on QCM Transducer and Acetylcholine Esterase Sensitive Film. *Micro Nano Lett.* **2017**, *12*, 113−116.

(20) Huang, P.-C.; Shen, M.-Y.; Yu, H.-H.; Wei, S.-C.; Luo, S.-C. Surface Engineering of Phenylboronic Acid-functionalized Poly(3,4-ethylenedioxythiophene) for Fast Responsive and Sensitive Glucose Monitoring. *ACS Appl. Bio Mater.* **2018**, *1* (1), 160−167.

(21) Fradkin, J. E.; Cowie, C. C.; Hanlon, M. C.; Rodgers, G. P. Celebrating 30 Years of Research Accomplishments of the Diabetes Control and Complications Trial/Epidemiology of Diabetes Interventions and Complications Study. *Diabetes* **2013**, *62* (12), 3963−3967.

(22) Toschi, E.; Slyne, C.; Atakov-Castillo, A.; Greenberg, J.; Greaves, T.; Carl, S. P.; Munshi, M. Use of Real Time Continuous Glucose Monitoring (CGM) in Real Life Clinical Practice Compared with Finger-Stick Glucose Monitoring. *Diabetes* **2018**, *67*, 959-P.

(23) Clarke, S. F.; Foster, J. R. A History of Blood Glucose Meters and Their Role in Self-Monitoring of Diabetes Mellitus. *Brit. J. Biomed. Sci.* **2012**, *69*, 83−93.

(24) Agrawal, R. P.; Sharma, N.; Rathore, M. S.; Gupta, V. B.; Jain, S.; Agarwal, V.; Goyal, S. Noninvasive Method for Glucose Level Estimation by Saliva. *J. Diabetes Metab.* **2013**, *4*, 1000266.

(25) Gupta, S.; Sandhu, S. V.; Bansal, H.; Sharma, D. Comparison of Salivary and Serum Glucose Levels in Diabetic Patients. *J. Diabetes Sci. Technol.* **2015**, *9*, 91−96.

(26) Soni, A.; Jha, S. K. Smartphone Based Non-Invasive Salivary Glucose Biosensor. *Anal. Chim. Acta* **2017**, *996*, 54−63.

(27) Ngamchuea, K.; Batchelor-McAuley, C.; Compton, R. G. Understanding Electroanalytical Measurements in Authentic Human Saliva Leading to the Detection of Salivary Uric Acid. *Sensor Actuat B-Chem.* **2018**, *262*, 404−410.

(28) Hu, S.; Loo, J. A.; Wong, D. T. Human Saliva Proteome Analysis and Disease Biomarker Discovery. *Expert Rev. Proteomics* **2007**, *4*, 531−538.

(29) Mahon, E.; Aastrup, T.; Barboiu, M. Dynamic Glycovesicle Systems for Amplified QCM Detection of Carbohydrate-Lectin Multivalent Biorecognition. *Chem. Commun.* **2010**, *46*, 2441−2443.

(30) Zheng, B.; Cheng, S.; Liu, W.; Lam, M. H.-W.; Liang, H. J. Small Organic Molecules Detection Based on Aptamer-Modified Gold Nanoparticles-Enhanced Quartz Crystal Microbalance with Dissipation Biosensor. *Anal. Biochem.* **2013**, *438*, 144−149.

(31) Samoei, G. K.; Wang, W. H.; Escobedo, J. O.; Xu, X. Y.; Schneider, H.-J.; Cook, R. L.; Strongin, R. M. A Chemomechanical Polymer that Functions in Blood Plasma with High Glucose Selectivity. *Angew. Chem. Int. Ed.* **2006**, *45*, 5319−5322.

(32) Norrild, J. C.; Søtofte, I. Design, Synthesis and Structure of New Potential Electrochemically Active Boronic Acid-Based Glucose Sensors. *J. Chem. Soc.* **2002**, *2*, 303−311.

(33) Suri, J. T.; Cordes, D. B.; Cappuccio, F. E.; Wessling, R. A.; Singaram, B. Continuous Glucose Sensing with a Fluorescent Thin-Film Hydrogel. *Angew. Chem. Int. Ed.* **2003**, *42*, 5857−5859.

(34) Mirmohseni, A.; Hassanzadeh, V. Application of Polymer-Coated Quartz Crystal Microbalance (QCM) as a Sensor for BTEX Compounds Vapors. *J. Appl. Polym. Sci.* **2001**, *79* (6), 1062−1066.

(35) Ma, H. W.; Hyun, J.; Stiller, P.; Chilkoti, A. "Non-Fouling" Oligo(ethylene glycol)-Functionalized Polymer Brushes Synthesized by Surface-Initiated Atom Transfer Radical Polymerization. *Adv. Mater.* **2004**, *16* (4), 338−341.

(36) Arakawa, T.; Kuroki, Y.; Nitta, H.; Chouhan, P.; Toma, K.; Sawada, S.-I.; Takeuchi, S.; Sekita, T.; Akiyoshi, K.; Minakuchi, S.; Mitsubayashi, K. Mouthguard Biosensor with Telemetry System for Monitoring of Saliva Glucose: A Novel Cavitas Sensor. *Biosens. Bioelectron.* **2016**, *84*, 106−111.

(37) Lu, X. L.; Mi, Y. L. Characterization of the Interfacial Interaction between Polyacrylamide and Silicon Substrate by Fourier Transform Infrared Spectroscopy. *Macromolecules* **2005**, *38*, 839−843.

https://dx.doi.org/10.1021/acsami.0c08229
ACS Appl. Mater. Interfaces 2020, 12, 34190−34197

(38) van Heijnsbergen, D.; Jaeger, T. D.; von Helden, G.; Meijer, G.; Duncan, M. A. The Infrared Spectrum of Al^+−benzene in the Gas Phase. *Chem. Phys. Lett.* **2002**, *364*, 345−351.
(39) Peng, H. F.; Ning, X. Y.; Wei, G.; Wang, S. P.; Dai, G. L.; Ju, A. Q. The Preparations of Novel Cellulose/Phenylboronic Acid Composite Intelligent Bio-Hydrogel and Its Glucose, pH-Responsive Behaviors. *Carbohydr. Polym.* **2018**, *195*, 349−355.
(40) Sugnaux, C.; Klok, H.-A. Glucose-Sensitive QCM-Sensors Via Direct Surface RAFT Polymerization. *Macromol. Rapid Commun.* **2014**, *35*, 1402−1407.
(41) NIST Standard Reference Database—B1s.
(42) Ye, G.; Wang, X. G. Glucose Sensing through Diffraction Grating of Hydrogel Bearing Phenylboronic Acid Groups. *Biosens. Bioelectron.* **2010**, *26*, 772−777.
(43) Gabai, R.; Sallacan, N.; Chegel, V.; Bourenko, T.; Katz, E.; Willner, I. Characterization of the Swelling of Acrylamidophenylboronic Acid-Acrylamide Hydrogels upon Interaction with Glucose by Faradaic Impedance Spectroscopy, Chronopotentiometry, Quartz-Crystal Microbalance (QCM), and Surface Plasmon Resonance (SPR) Experiments. *J. Phys. Chem. B* **2001**, *105*, 8196−8202.
(44) Vinita; Nirala, N. R.; Tiwari, M.; Prakash, R. A Nanoporous Palladium (II) Bridged Coordination Polymer Acting as a Peroxidase Mimic in a Method for Visual Detection of Glucose in Tear and Saliva. *Microchim. Acta* **2018**, *185*, 245.
(45) Dai, J. X.; Zhao, H. R.; Lin, X. Z.; Liu, S.; Fei, T.; Zhang, T. Design Strategy for Ultrafast-Response Humidity Sensors Based on Gel Polymer Electrolytes and Application for Detecting Respiration. *Sensor Actuat B-Chem.* **2020**, *304*, 127270.
(46) Fang, H.; Lin, J. B.; Hu, Z. X.; Liu, H.; Tang, Z. R.; Shi, T. L.; Liao, G. L. $Cu(OH)_2$ Nanowires/Graphene Oxide Composites Based QCM Humidity Sensor with Fast-Response for Real-Time Respiration Monitoring. *Sensor Actuat B-Chem.* **2020**, *304*, 127313.
(47) Dentistry−Corrosion Test Methods for Metallic Materials. ISO 10271:2011.
(48) Lazerges, M.; Perrot, H.; Rabehagasoa, N.; Compère, C. Thiol- and Biotin-Labeled Probes for Oligonucleotide Quartz Crystal Microbalance Biosensors of Microalga Alexandrium Minutum. *Biosensors* **2012**, *2* (3), 245−254.
(49) Vejayakumaran, P.; Rahman, I. A.; Sipaut, C. S.; Ismail, J.; Chee, C. K. Structural and Thermal Characterizations of Silica Nanoparticles Grafted with Pendant Maleimide and Epoxide Groups. *J. Colloid Interf Sci.* **2008**, *328* (1), 81−91.

https://dx.doi.org/10.1021/acsami.0c08229
ACS Appl. Mater. Interfaces 2020, 12, 34190−34197